



UMR-MEC Conference on Energy


---

09 Oct 1975

## Wind Energy Concentrators

John L. Loth

Follow this and additional works at: <https://scholarsmine.mst.edu/umr-mec>

 Part of the [Electrical and Computer Engineering Commons](#), [Mechanical Engineering Commons](#), [Mining Engineering Commons](#), [Nuclear Engineering Commons](#), and the [Petroleum Engineering Commons](#)

---

### Recommended Citation

Loth, John L., "Wind Energy Concentrators" (1975). *UMR-MEC Conference on Energy*. 65.  
<https://scholarsmine.mst.edu/umr-mec/65>

This Article - Conference proceedings is brought to you for free and open access by Scholars' Mine. It has been accepted for inclusion in UMR-MEC Conference on Energy by an authorized administrator of Scholars' Mine. This work is protected by U. S. Copyright Law. Unauthorized use including reproduction for redistribution requires the permission of the copyright holder. For more information, please contact [scholarsmine@mst.edu](mailto:scholarsmine@mst.edu).

## WIND ENERGY CONCENTRATORS\*

John L. Loth  
West Virginia University  
Department of Aerospace Engineering  
Morgantown, West Virginia 26506

### Abstract

This paper presents two alternatives to the shrouded propeller wind energy concentrator. Their operation is based on generating a low pressure area, with high local wind velocity, around the windmill rotor.

The two types of wind energy concentrators considered are: (1) the "obstruction type" concentrator where a vertical cylinder or vertical flat surface is used to produce high local velocities around two counter-rotating vertical axis rotors, and (2) the "vortex type" concentrator where a horizontal vortex is generated by a vertical high lift wing of finite span. The high local wind kinetic energy inside the vortex is harnessed by a horizontal axis rotor.

The performance parameters such as the power concentration ratio and the associated area ratio have been determined theoretically. Some preliminary experimental data are included.

### Nomenclature

a	= radius of maximum rotational velocity in vortex	S	= concentrator wing area = bc.
A	= dimensionless total concentrator plus turbine area = $1 + \frac{4S}{\pi d^2}$ .	$U_\infty$	= free wind velocity.
$\bar{A}$	= wing aspect ratio $2b/c$ .	V	= local velocity.
b	= semi wing span.	$V_{av}$	= average velocity at rotor inlet.
c	= mean aerodynamic wing chord.	$V_\theta$	= vortex tangential velocity.
$C_L$	= average wing lift coefficient.	$V_{\theta av}$	= average vortex tangential velocity at rotor inlet.
$c_p$	= pressure coefficient based on free wind speed.	w	= width of two dimensional concentrator.
$c_{pav}$	= average pressure coefficient around windmill rotor.	Z	= ratio of induced drag to free wind kinetic energy at turbine inlet.
$D_i$	= semi wing span induced drag.	$\Gamma_o$	= bound vortex strength.
d	= windmill rotor diameter.	$\delta$	= boundary layer thickness.
e	= span wise loading efficiency factor.	$\rho$	= density.
f	= rate of vortex rotational kinetic energy passing through an area with diameter d and divided by $D_i$ .		
K.E.	= kinetic energy.		
p	= pressure.		
R	= wind power concentration ratio.		
r	= radius in vortex.		

### INTRODUCTION

The search for finding more economical methods for harnessing available wind power has found renewed interest in view of the rising fuel costs. Commercial type wind power generating stations must be large in size because of the generally low density of the wind

\*Research in part funded by NSF Grant Number: AER 7500367-000

kinetic energy. This results in a low power output per square foot of wind machine. The existing commercial type wind power generating stations require large rotor frontal areas with high capital investment and maintenance cost. A large rotating rotor might not be aesthetic in appearance and the environmental impact of wind power generating stations may limit their use. These problems might be reduced if the available wind energy is concentrated locally by either natural or man-made nonrotating objects, such as mountain tops, mountain passes, corners of buildings, the top of a sloping wall, etc.

None of these natural or man-made wind energy concentrators increase the total pressure of the wind, but they create an area of low pressure around the windmill rotor. The local wind kinetic energy increases in this area of low pressure and the amount of wind power harnessed per square foot of the rotor area can be increased two to five fold. This increase is named the concentration ratio  $R$ . The area of low pressure around the rotor can be created by a non-rotating wind energy concentrator adjacent to the rotor. The area of low pressure around the rotor should be exposed to the incoming wind with a minimum of viscous losses. None of these nonrotating wind energy concentrators increase the stagnation pressure of the wind. Only the dynamic pressure is increased locally by lowering the static pressure around the rotor. There are basically three methods by which a local area of low pressure can be generated.

(1) A mountain pass, when aligned with the wind experiences a venturi effect with high velocity in the narrow passage. Shrouded windmill propellers are designed to operate on the same principle with the rotor placed at the minimum area inside the shroud, see Reference 1 and Figure 1. The flow passage must be properly aligned with the direction of the wind. The wind energy concentrators based on this principle are here referred to as "Venturi Types."

(2) Single mountain peaks present an obstruction to the flow. The air is forced to deflect and flow around the obstruction. The resulting flow curvature sets up a pressure gradient perpendicular to the surface and creates high and low pressure regions on the windward side of the mountain. The flow around a cylinder at the point of maximum cross section, would speed up to twice the wind velocity if the flow were inviscid. In a real fluid the point of maximum velocity occurs slightly upstream of the maximum cross section. A flat plate placed perpendicular to the wind

also experiences a very low pressure near the edges (see Figure 2 taken from Reference 2). Note the cylinder can remain stationary but the rotors and the optional flat plate sections must align themselves with the wind direction. The wind energy concentrators based on this principle are here referred to as "Obstruction Types".

(3) Tornadoes are vortex type rotational flows. The curvature of the flow sets up a radial pressure gradient which results in a low pressure region in the center of the vortex. One can also think of the centrifugal force creating the vacuum in the core of the vortex.

Vertical vortices like tornadoes lack the high axial velocity and flow required for high power extraction. Some power could be extracted if the tornado was kept stationary, and air was ducted through a turbine and exhausted in the low pressure core of the vortex. The inlet of the duct should align itself with the direction of the wind so as to get maximum total pressure at the inlet of the turbine.

Horizontal vortices like those trailing behind the wing tips of an aircraft have a similar low pressure region in the core, but in addition, also a high axial velocity and mass flow rate in the core of the vortex. Due to viscous effects the velocities in the core of the vortex are limited (see Figure 3). The wind blowing over a finite length stationary wing can convert a great deal of its kinetic energy to generating a wing tip vortex with a low pressure in its center (see Figure 4). The wind energy concentrators based on this principle are here referred to as "Vortex Types". The trailing vortex system, shed from aircraft wings, has been treated extensively in the literature. (3) (4)

These vortices are created by the cross flow around the tip of a straight wing or the leading edge of a swept wing. The cross flow goes from the high pressure bottom surface of the wing to its low pressure upper surface. The corner of a building facing the wind experiences similar leading edge vortices as a swept wing. An excellent flow visualization of these vortices is shown in Reference 2 and reproduced here as Figure 5. The angle of attack of the flat roof is created by the upward flow deflection as the wind has to flow over and around the building.

Of the three types of wind energy concentrators outlined above, only the symmetric "Obstruction Type" in combination with one or more vertical windmill rotors can be utilized as a stationary wind energy concentrator (see Figure 6). All other types of wind energy

concentrators have to align themselves with the wind direction.

Both the "Obstruction Type" and the "Vortex Type" wind energy concentrators are under development at West Virginia University. An overview of their performance limitations in terms of wind power concentration ratio  $R$  and associated total area ratio  $A$  is presented herein. The power concentration ratio  $R$  does not incorporate the efficiency with which power is harnessed by the windmill rotor. The power concentration ratio  $R$  is defined as the increase in kinetic energy flow rate per unit area. If one compares a conventional windmill rotor with a rotor operating in conjunction with a nonrotating wind energy concentrator, then the rotor must be reduced in area by the ratio  $R$  in order to have the same rate of inflow of wind energy as the conventional rotor.

The total projected area of the nonrotating concentrator and that of the rotor is designated by  $A$  when nondimensionalized by the rotor area. Therefore, the total projected area of the concentrator and the rotor is  $A/R$  times greater than the conventional rotor projected area.

#### POWER CONCENTRATION LEVEL

As was mentioned before, none of these wind energy concentrators increase the total pressure of the wind, but they create an area of low pressure and therefore, high local wind kinetic energy available for harnessing. The magnitude of the low pressure obtained is usually expressed by a pressure coefficient:  $c_p = \frac{p - p_\infty}{\frac{1}{2} \rho U_\infty^2}$  where  $p$  is the local static pressure and  $p_\infty$ ,  $\rho$ ,  $U_\infty$  are the undisturbed wind static pressure, density, and velocity. Viscous effects have a major influence on the generation, magnitude, and location of the low pressure area. However, only a small portion of such a low pressure area suffers total pressure loss due to viscous effects and usually most of the wind energy can be extracted in the low pressure area with nearly inviscid flow. For inviscid incompressible flow the pressure coefficient  $c_p$  is related to the local velocity by the Bernoulli equation:  $c_p = 1 - (\frac{V}{U_\infty})^2$ . The wind energy concentrator produces a power concentration ratio which can be expressed as a function of the average value of both the pressure coefficient  $c_{pav}$  and velocity  $V_{av}$  at the rotor inlet.

Consider first the "Obstruction Type" concentrator with one or more rotors placed in the local low pressure area. Assume the velocity  $V_{av}$  to be an

average local inviscid velocity at the rotor inlet. The local wind power density available for harnessing is given by the kinetic energy times the mass flow per unit area  $= \rho V_{av} (\frac{V_{av}^2}{2})$ . Without wind energy concentrator the power density available  $= \rho U_\infty (\frac{U_\infty^2}{2})$ . Thus the power concentration ratio  $R$ , defined as the ratio of power densities is:

$$R(\text{obstruction type}) = \left( \frac{V_{av}}{U_\infty} \right)^3 \approx (1 - c_{pav})^{3/2}$$

Note that if all the kinetic energy  $(\frac{U_\infty^2}{2})$  would be harnessed then the mass flow through the rotor  $\propto \rho U_\infty$  and the power output would reduce to zero. Consequently, for maximum power output one can only harness a portion of the available kinetic energy with the obstruction type concentrator. For unseparated flow over a cylinder as in Figure 2A, the theoretical maximum value is  $V=2U_\infty$  or  $R=(2)^3=8$ . Due to actual flow separation  $R$  will be limited to about 4.

Next consider the "Vortex Type" concentrator. A rotor, placed coaxial with the vortex axis is used to harness both rotational and axial kinetic energy in the vortex. Assume inviscid flow and  $V_{\theta av}$  to be the average tangential velocity at the rotor inlet and approximate the axial velocity by  $U_\infty$ . The average pressure coefficient is  $c_{pav} = 1 - \left( \frac{V_{\theta av}^2 + U_\infty^2}{U_\infty^2} \right)$ . At the rotor inlet the wind power density available for harnessing is given by the kinetic energy times the mass flow rate per unit area  $= \rho U_\infty \left( \frac{V_{\theta av}^2 + U_\infty^2}{2} \right)$ . Note for the

vortex type concentrator all the rotational kinetic energy  $\frac{V_{\theta}^2}{2}$  can be harnessed without reducing the mass flow through the rotor. Without wind energy concentrators, the power density  $= \rho U_\infty (\frac{U_\infty^2}{2})$ . Thus the power concentration ratio defined as the ratio of power densities is:

$$R(\text{vortex type}) = \frac{V_{\theta}^2}{U_\infty^2} \approx 1 - c_{pav}$$

Viscosity limits the magnitude of  $c_p$  in the vortex. Experimental values of  $c_p$  in the vortex over a building roof are shown in Figure 5. This is similar to the trailing vortices shed from a delta wing with low aspect ratio; see Reference 5.

The magnitude of the pressure coefficients measured inside the trailing vortices is nearly linearly proportional to the wing lift coefficient  $C_L^{2/e}$ . Low aspect ratio wings, have a low maximum lift coefficient and correspondingly limited magnitude of  $c_p$  and  $R$ . Medium and high aspect ratio straight wings, see Reference 6, can generate high lift coefficients and

therefore, large magnitudes of both the pressure coefficient inside the vortex and the power concentration ratio  $R$ . The application of inverse wing taper and twist can generate more uniform spanwise loading and further increase the lift coefficient of the wing. Aircraft do not use this because the associated increase in induced drag  $D_i$  has to be overcome by engine thrust. Vortex type wind energy concentrators benefit two ways from more uniform spanwise wing loading. First it increases  $C_L$  and  $R$  as mentioned above and secondly most of the trailing vorticity will shed near the wing tip so that it rolls up more rapidly into a single vortex.

#### OBSTRUCTION TYPE CONCENTRATORS

A few possible configurations of "Obstruction Type" concentrators in combination with two Savonius rotors are shown in Figures 6, 7, and 8. Figure 6 shows a cylindrical type concentrator. Due to the symmetry of the cylinder it can remain stationary for all wind directions: Two counter-rotating windmill rotors are placed in the areas of minimum pressure, the location of which depends on the wind direction. Thus the rotor bearings have to be mounted on a pivot system which orients itself to the wind direction (see Figure 9). Small scale wind tunnel experiments conducted at WVU showed that the indicated direction of rotation of the rotors produced slightly higher power concentration than when they are reversed. Placing the rotors slightly forward of the  $90^\circ$  position was found to be optimum, and the rotors should be kept outside the boundary layer thickness  $\delta$ . Another configuration tested was the pivoting flat surface as shown in Figure 7. A slight improvement was noticed while using sharp corners. A combination of a pivoting flat surface and a stationary cylinder is shown in Figure 8. The WVU wind tunnel model uses a belt drive system as shown in Figure 9, to couple the two rotors; this eliminated the rpm fluctuations of the individual rotors, which was measured by a tach-generator. The tunnel dynamic head was measured with a pressure transducer with digital display. The wind tunnel blockage and the rotor rpm and torque were maintained constant for both tests, with the cylinder in place and with the cylinder moved six rotor diameters downstream. Then, for these two cylinder positions the wind tunnel dynamic heads were compared. By assuming the rotor efficiency and thus the power available at the rotor to be the same for both tunnel speeds, one can compute the power concentration ratio  $R$  from the third

power of the tunnel velocity ratio, see Figure 10. Only two cylinder diameters and one rotor diameter were tested at WVU. Consequently only two test points are shown. Each point represents the average value of  $R$  over a wide range of tunnel speeds.

#### VORTEX TYPE CONCENTRATOR

Any finite lifting wing has associated with it a bound vorticity which varies in strength along the span. All this vorticity is shed in the form of a trailing vortex sheet. The spanwise intensity of the trailing vorticity is proportional to the rate of change in spanwise wing loading.

A wing with inverse taper and twist and thus nearly uniform spanwise loading has nearly all the trailing vorticity shed near the wing tip. The trailing vorticity rolls up, at each wing tip, into a strong vortex with its axis in the direction of the free stream. The rate of roll up of the vortex sheet can be computed as a function of wing loading as is shown in Reference 7. In the case of an elliptically loaded wing, as much as 40% of the vortex sheet is rolled up into a single vortex at one chord length downstream of the trailing edge. For a wing loaded nearly uniformly along its span, almost all of the vorticity will be rolled up at that distance. The trailing vortex system induces a downwash velocity on the bound-vortex in the wing, which results in an induced drag, designated by  $D_i$  for a semi-span wing. Due to the high stability of the trailing vortex system, the vortex rotational velocities can still be measured hundreds of wing spans downstream. Experimental data for the far field vortex system are given in Reference 3. The following numerical quantities are computed using these data. Even in the far field the axial momentum deficit in the vortex is small and accounts for less than 10% of the induced drag. More than 90% of the induced drag is in the form of a pressure drag created by the vacuum in the vortex. Centrifugal effects in the rotating vortex maintain this vacuum up to great distances from the vortex core. The core is in near solid body rotation and defined by the maximum tangential velocity  $V_{\theta_{max}}$  at radius  $(a)$ . Significant viscous effects extend to about 4.5 times the core radius from the center and the circulation at radius  $(a)$  is only about half that in the irrotational part of the vortex.

Only 16% of the induced drag is due to the vacuum level in the viscous region, while 74% of the induced drag is due to vacuum in the near inviscid irrotation-

al part of the vortex. It is interesting to note that inside the irrotational outer part of the vortex, the pressure drag due to the vacuum equals the local rotational kinetic energy, which can be derived from the Bernoulli equation. However, inside the viscous region of the vortex the rotational kinetic energy is only 63% of the pressure drag due to vacuum in that region. Therefore, only 84% of the induced drag manifests itself in the form of rotational energy of the wing tip vortex. Similar numbers can be obtained by using analytical models of Newman<sup>(8)</sup> or Batchelor.<sup>(9)</sup> A wind turbine with an impulse type rotor can be used to harness the rotational vortex kinetic energy captured. The amount of vortex rotational kinetic energy entering the turbine depends on its diameter  $d$  and has been computed as a fraction  $f$  of  $D_i$  as shown in

Figure 11:

$$f = \frac{\int_0^{\frac{d}{2}} \frac{1}{2} \rho V_{\theta}^2 2\pi r dr}{D_i} = \frac{\text{vortex rotational K.E.}}{\text{semispan induced drag}}$$

To compute the power concentration ratio, one needs to define  $Z$  as the ratio of the induced drag to the free wind kinetic energy in a streamtube of cross-sectional area equal to that of the turbine inlet.

$$Z = \frac{D_{i=\frac{1}{2}\rho U_{\infty}^2 C_{D_i} bc}}{\frac{1}{2}\rho U_{\infty}^2 \frac{\pi}{4} d^2} = \frac{C_{D_i} AR}{\frac{\pi}{2} (\frac{d}{c})^2} = \left(\frac{C_L}{e}\right)^2 \left(\frac{1}{\frac{\pi}{2} (\frac{d}{c})^2}\right)$$

Here  $e$  is the spanwise loading efficiency, which should be as small as possible. The power concentration ratio  $R$  can then be computed from:

$$R = \frac{\text{axial wind K.E.} + \text{rotational K.E.}}{\text{free wind K.E.}} = 1 + f \cdot Z$$

The corresponding total area ratio of wing concentrator plus turbine, to that of the turbine is given by

$$A = \frac{bc + \frac{\pi}{4} d^2}{\frac{\pi}{4} d^2} = 1 + \frac{2 AR}{\pi (\frac{d}{c})^2}$$

Both  $R$  and  $A$  have been computed for a uniformly loaded high lift semi-span wing with the turbine placed at a distance of one mean aerodynamic chord downstream of the trailing edge and concentric with the vortex centerline. The vortex core radius  $a/c$  at that location is found from experiments to be .03. Using this value one can proceed to compute  $f$ ,  $Z$ , and  $R$  as a function of  $C_L^2/e$  and turbine diameter  $d/c$ . The results are plotted in Figure 12 for various values of  $C_L^2/e$ . To get high values of  $R$  it is essential that one needs high lift coefficients, which means also a high aspect ratio. Unfortunately, as the aspect ratio increases, the corresponding area ratio  $A$  increases.

To find the optimum aspect ratio which controls both  $R$  and  $A$  one must perform an economic tradeoff study. The maximum value of  $R$  is found for  $d = 3a$ , then  $R$  can be computed to be

$$R_{\max} = 1 + \frac{2}{3} \left(\frac{V_{\theta \max}}{U_{\infty}}\right)^2 \approx 1 + .24 C_{p_{\min}} \approx 1 + .5 C_L^2 / e.$$

Because  $a/c$  is small, the maximum value of  $R$  has a high area ratio associated with it.

A shroud around the turbine is recommended to stabilize the vortex and to maintain the low pressure at the turbine outlet even after the rotational velocity has been harnessed. The presence of the turbine will have an adverse effect on the obtainable maximum lift coefficient of the wing. Using lifting line theory it is estimated that the presence of the turbine at a distance of 1 chord length downstream reduces  $C_L^2/e$  by 13%. In Figure 13 is shown a model of a high lift wing vortex type concentrator. The airfoil chosen was a modified Liebeck airfoil as is described by Smith.<sup>(10)</sup> It is anticipated that the addition of a Gurney flap and turbulence generators might create a maximum lift coefficient  $C_L=4.0$  or better. However, the associated high drag might increase the blockage effect and lower the effective free wind speed. It is expected that with an aspect ratio  $AR=5$  and a turbine diameter of  $.75c$  one can achieve a concentration ratio  $R=2.5$  and a corresponding area ratio  $A=6.5$ . Note that  $R$  does not reflect the higher efficiency with which rotational kinetic energy can be harnessed as compared to axial kinetic energy.

## CONCLUSIONS

All wind energy concentrators mentioned herein such as "Venturi Types," "Obstruction Types," and "Vortex Types" operate on the same principle. They are non-rotating and generate an area of low pressure and high kinetic energy in which the rotor is placed. The application of a concentrator permits a reduction in rotor area by an amount  $R$  without change in power output. The total area of the concentrator plus rotor is then  $A/R$  larger than the original rotor where  $A$  is larger than  $R$ .

The application of a concentrator is governed by the economic and aesthetic tradeoffs. In many designs the concentrator finds additional use as support structure for the rotor and generator. Rotors operating in conjunction with a concentrator have a smaller diameter and torque but a higher angular velocity; this may produce savings in gearbox and transmission costs. The obtainable power concentration ratio  $R$  varies

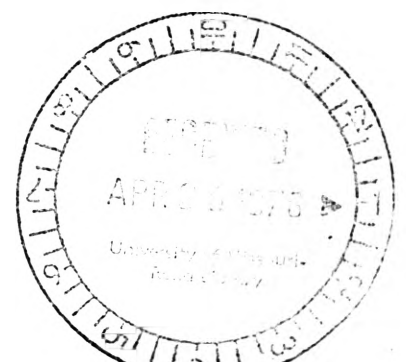
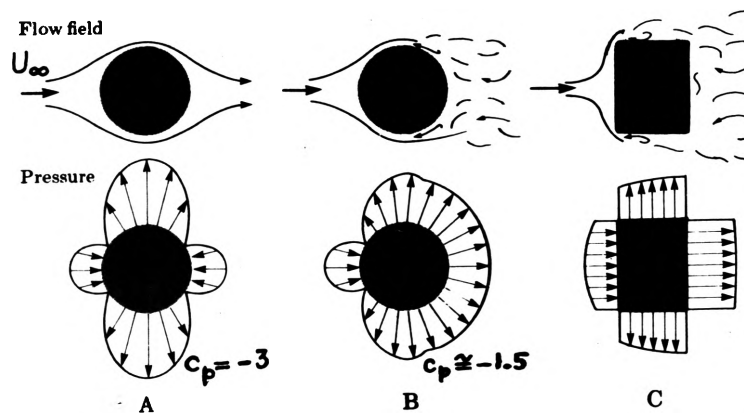
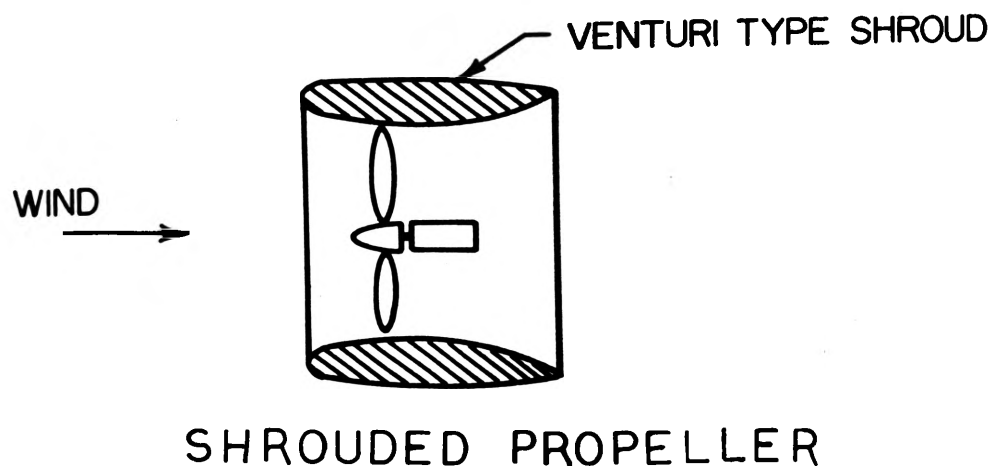
between 2 and 4 and the corresponding area ratio A varies between 3 and 10. At this stage no clear cut advantages are shown by one concentrator over the others. The few encouraging results justify a continued effort in the development of new economical and efficient wind energy concentrators and improving the existing ones.

#### REFERENCES

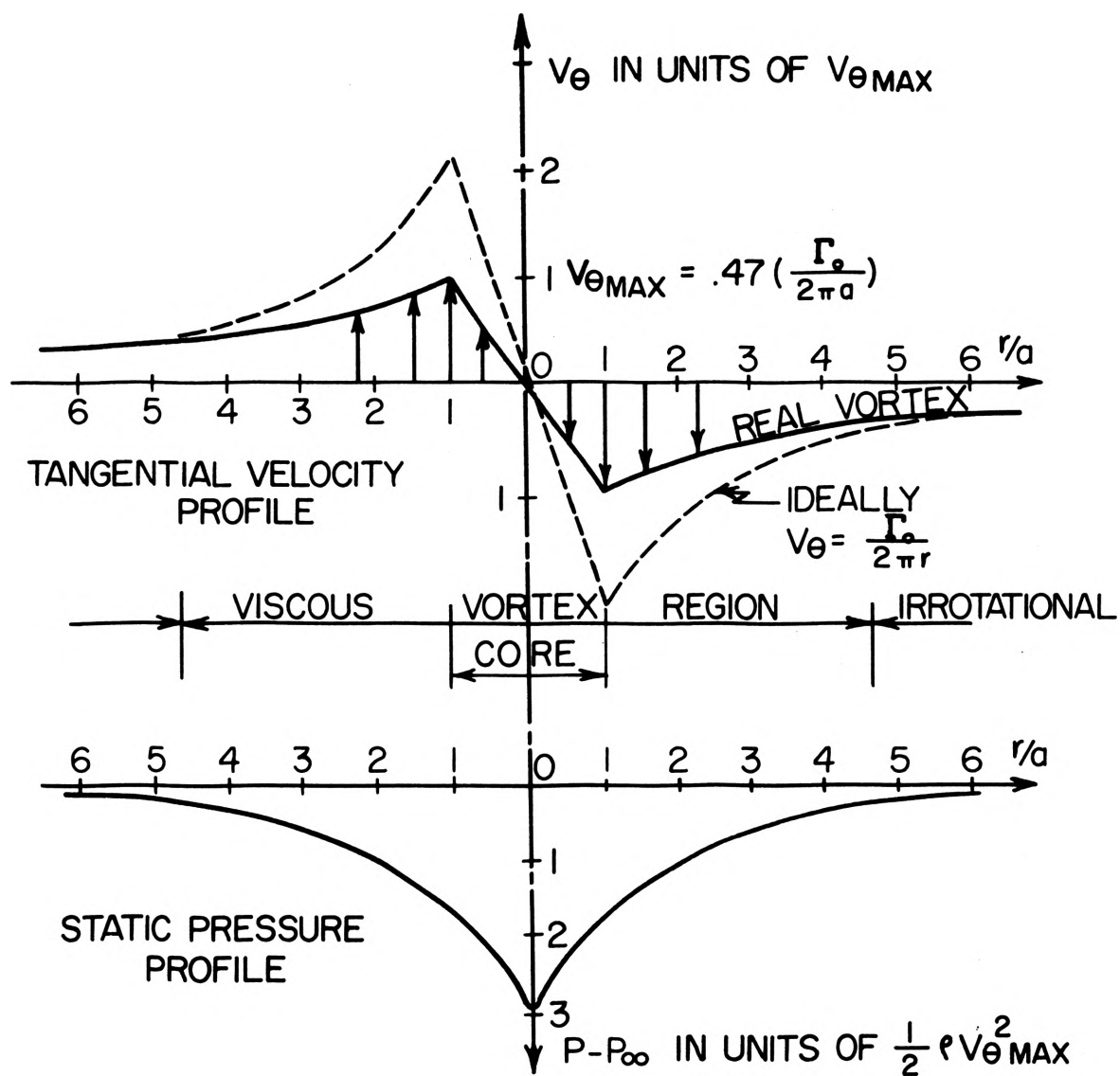
- (1) Oman, R., "Cost Effective Diffuser Augmentation of Wind Turbine Power Generators," Grumman Aerospace, ERDA & NSF Wind Energy Workshop, June, 1975.
- (2) Thomann, H., "Wind Effects on Buildings and Structures," American Scientist, Vol. 63, May-June, 1975.
- (3) Ciffone, D. L. and Orloff, K. L., "Far-Field Wake-Vortex Characteristics of Wings," Journal of Aircraft, Vol. 12, No. 5, 1975.
- (4) Chiger, N. A., "Vortexes in Aircraft Wakes," Scientific American, Vol. 230, No. 3, 1974.
- (5) Sforza, P., "Vortex Augmentor Concepts for Wind Energy Conversion," Polytechnic Institute of New York, ERDA & NSF Wind Energy Workshop, June, 1975.
- (6) Walters, R. E., "Innovative Vertical-Axis Wind Machines," West Virginia University, ERDA & NSF Wind Energy Workshop, June, 1975.
- (7) Wilson, J. D. and Loth, J. L., "Real Time Development of the Wake of a Finite Wing," TR-23, Department of Aerospace Engineering, West Virginia University, February, 1974.
- (8) Newman, B. G., "Flow in a Viscous Trailing Vortex," Aeronautical Quarterly, June, 1958.
- (9) Batchelor, G. K., "Axial Flow in Trailing Line Vortices," J. Fluid Mech., Vol. 20, Part 4, 1964.
- (10) Smith, A. M. O., "High Lift Aerodynamics," Journal of Aircraft, Vol. 12, No. 6, June, 1975.

#### BIOGRAPHY

John L. Loth, born 1933, The Netherlands. Undergraduate degree in Mechanical Engineering, 1955 Amsterdam. M.S. and Ph.D. 1962 University of Toronto. Teaching Experience: University of Illinois 1962-1967, West Virginia University 1967-present. Research and consulting in areas of aircraft propulsion, flight testing, fluid flow and low speed aerodynamics.

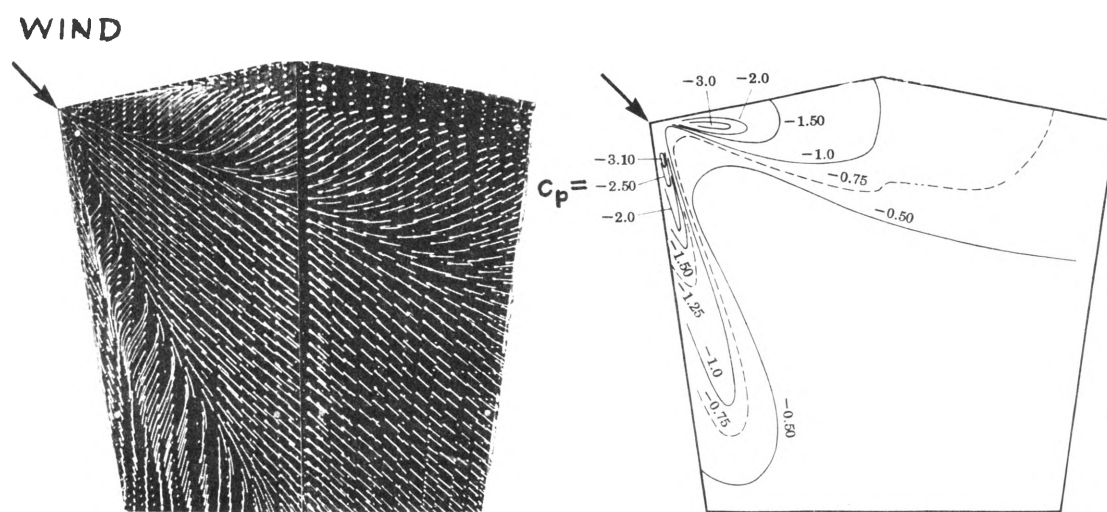




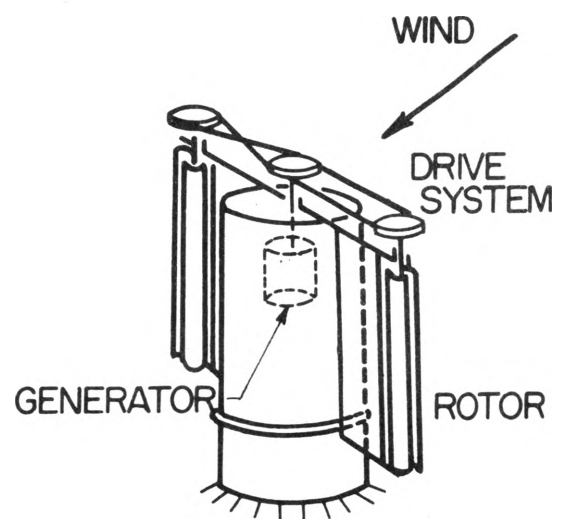
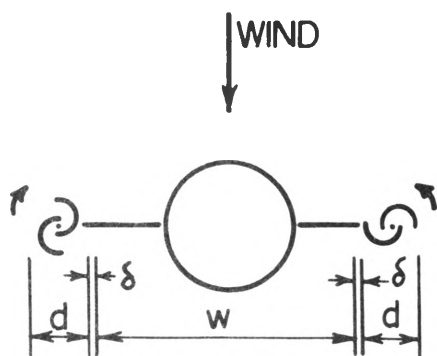
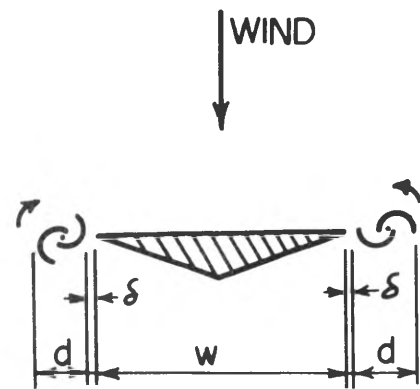
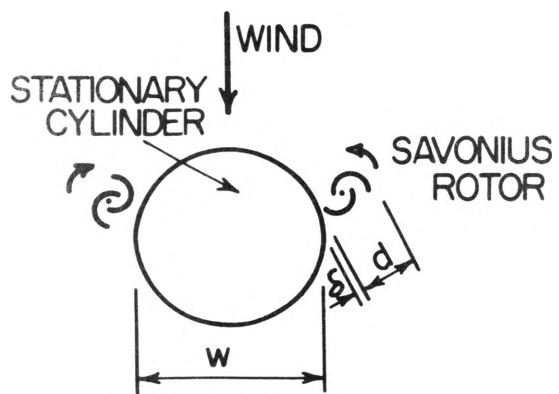


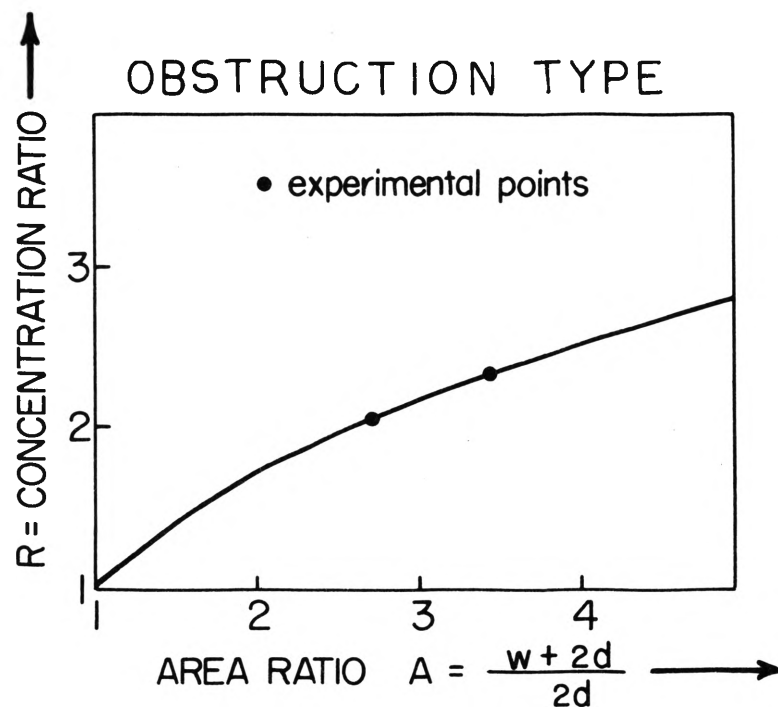
TYPICAL VORTEX PROFILES

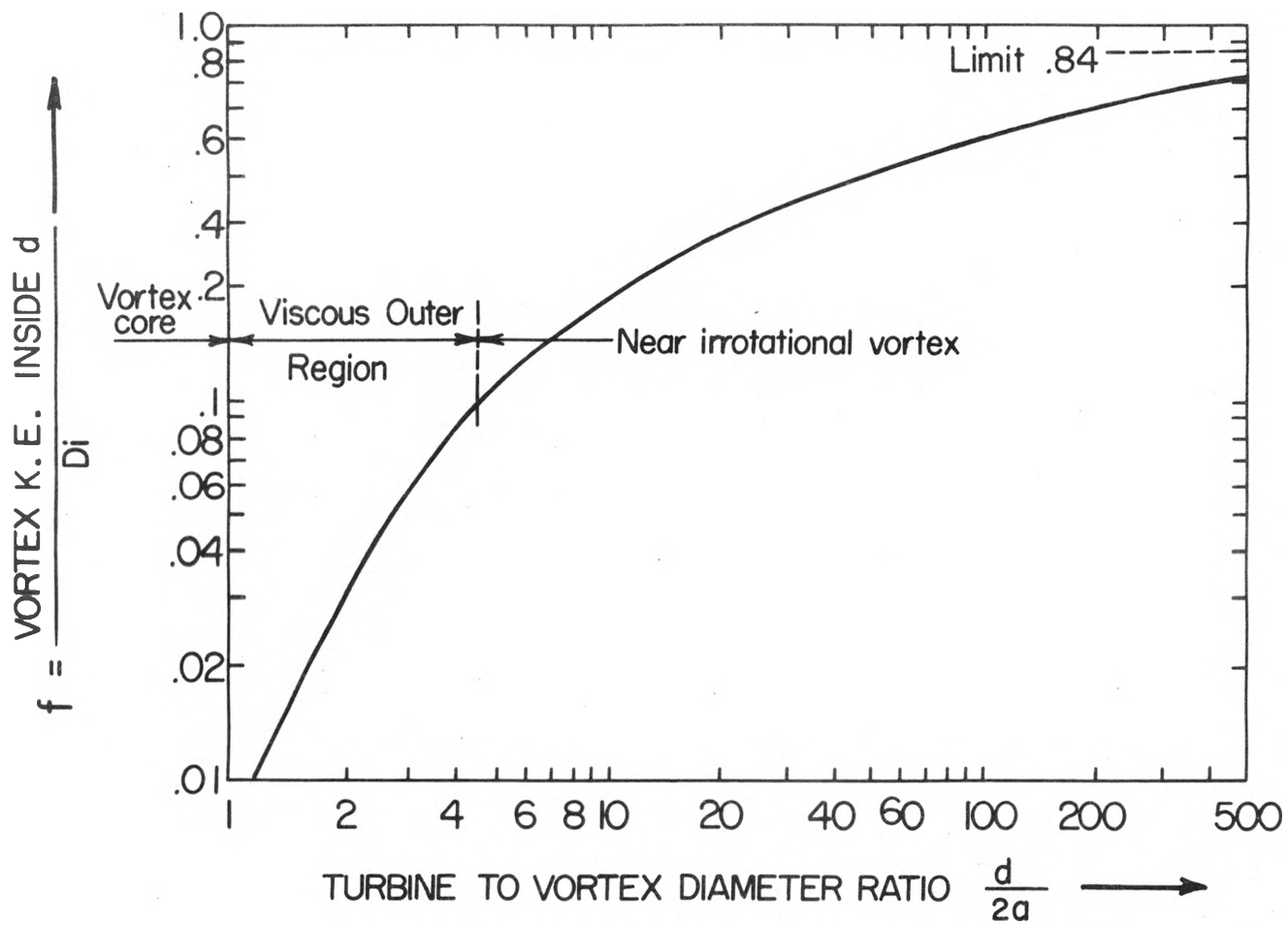




# VORTICES ON BUILDING ROOF







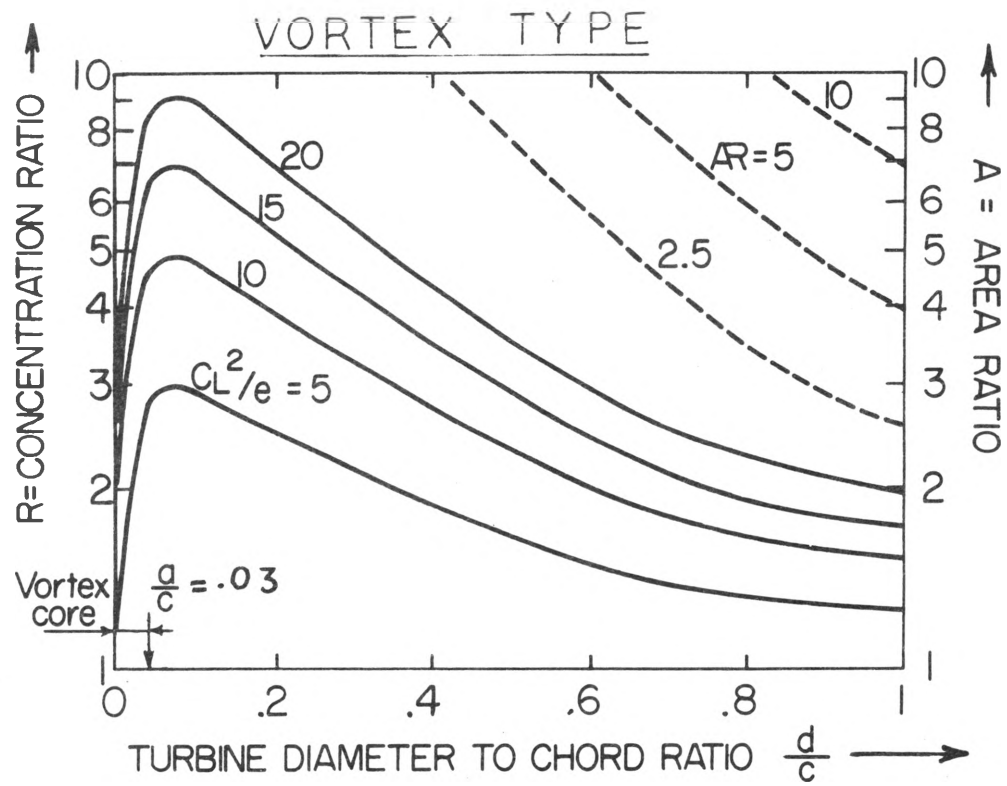




Fig. 13. "Vortex Type" wind energy concentrator model, using a high lift Liebeck type airfoil and a shrouded rotor.